Formation and Decomposition of Chemically Activated Cyclopentoxy Radicals from the c-C_5H_9 + O Reaction†

Karlheinz Hoyermann,‡ Jörg Nothdurft,*,‡ Matthias Olzmann,§ Jens Wehmeyer,‡ and Thomas Zeuch‡

Institut für Physikalische Chemie, Georg-August-Universität, Tammanstr. 6 D-37077 Göttingen, Germany, and Institut für Physikalische Chemie, Universität Karlsruhe, Kaiserstr. 12, D-76128 Karlsruhe, Germany

Received: August 15, 2005; In Final Form: October 18, 2005

The formation and the decomposition of chemically activated cyclopentoxy radicals from the c-C_5H_9 + O reaction have been studied in the gas phase at room temperature. Two different experimental arrangements have been used. Arrangement A consisted of a laser-flash photolysis set up combined with quantitative Fourier transform infrared spectroscopy and allowed the determination of the stable products at 4 mbar. The c-C_5H_9 radicals were produced via the reaction c-C_5H_{10} + Cl with chlorine atoms from the photolysis of $CFCl_3$; the O atoms were generated by photolysis of SO_2. Arrangement B, a conventional discharge flow-reactor with molecular beam sampling, was used to determine the rate coefficient. Here, the hydrocarbon radicals (c-C_5H_9, C_2H_5, CH_2OCH_3) were produced via the reaction of atomic fluorine with c-C_5H_{10}, C_2H_6, and CH_3-OCH_3, respectively, and detected by mass spectrometry after laser photoionization. For the c-C_5H_9 + O reaction, the relative contributions of intermediate formation (c-C_5H_9O*) and direct abstraction (c-C_5H_8 + OH) were found to be 68 ± 5 and 32 ± 4%, respectively. The decomposition products of the chemically activated intermediate could be identified, and the following relative branching fractions were obtained: c-C_5H_8O + H (31 ± 2%), $CH_2CH(CH_2)_2CHO$ + H (40 ± 5%), 2 C_2H_4 + H + CO (17 ± 5%), and C_3H_4O + C_2H_4 + H (12 ± 5%). Additionally, the product formation of the c-C_5H_8 + O reaction was studied, and the following relative yields were obtained (mol %): C_2H_4, 24%; C_3H_4O, 18%; c-C_5H_8O, 30%; c-C_5H_8O, 23%; 4-pentenal, 5%. The rate coefficient of the c-C_5H_9 + O reaction was determined relative to the reactions C_2H_5 + O and CH_3OCH_2 + O leading to $k = (1.73 \pm 0.05) \times 10^{14}$ cm^3 mol^{-1} s^{-1}. The experimental branching fractions are analyzed in terms of statistical rate theory with molecular and transition-state data from quantum chemical calculations, and high-pressure limiting Arrhenius parameters for the unimolecular decomposition reactions of C_5H_9O species are derived.

Introduction

The kinetic behavior of oxygenated hydrocarbon radicals such as alkoxy radicals is of interest in a variety of chemical processes. Only two aspects should be mentioned here in some detail: (i) The radical-induced polymerization on a technical scale is often induced by oxygen-centered radicals formed by thermal or photochemical decomposition of suitable initiators such as peroxides or peroxy esters. Besides the chain initiation step, RO + monomer, the alkoxy radical can undergo C−C and C−H bond scission as well as isomerization and change the character from an O-centered to a C-centered radical. The implications of these transformations on the initiator efficiency and the overall process of polymerization are discussed in a recent paper by Buback et al.[1] (ii) Alkoxy radicals are important intermediates in the mechanism of hydrocarbon oxidation under atmospheric as well as combustion conditions. At high temperatures, the hydrogen abstraction from alkanes by atoms (H, O) and radicals (OH, CH_3) leads to alkyl radicals (R), which then undergo thermal dissociation to smaller species or bimolecular reactions with atoms and other radicals. Although the concentration of O atoms is often distinctly below the concentration of O_2, the R + O reaction can become dominant under fuel-lean conditions as its rate coefficient for many radicals exceeds the rate coefficient of R + O_2 by several orders of magnitude. Detailed mechanisms for the combustion of alkanes and alkenes can be found in the literature.[2−6]

Recently, the scientific interest is increasingly directed to cycloalkanes (c-C_5H_{10}, c-C_6H_{12}), since they form a major class of components in different fuels. Thereby cyclic alkanes are important components of kerosene (Jet A, Jet A-1, JP-8).[7] Moreover, the total cycloalkane content can be up to 18% in fuel oils and up to 54% in diesel fuels.[8] As hydrogen abstraction from cycloalkanes leads to cyclic alkyl radicals, their reactions with O and O_2 are important.

Unimolecular reactions of alkoxy radicals have been extensively studied both experimentally and theoretically. The decomposition of thermally[9−12] and chemically activated radicals was investigated, and possible reaction paths were characterized by quantum chemical methods.[1,13−16] For the production of chemically activated RO, mainly the reaction R + O,[13−15,17,18] but in some cases also the reactions R + O_3[18,22] and R + NO_3[18] were used. To date, the kinetics of the following primary alkoxy

† Part of the special issue "Jürgen Troe Festschrift".

* To whom correspondence should be addressed. Fax: +49 551 393117. E-mail address: jnothdu@gwdg.de.

‡ Georg-August-Universität.

§ Universität Karlsruhe.

10.1021/jp054578c CCC: $33.50
Published on Web 11/16/2005

radicals has been studied: C_2H_5O,[17,18,19,20] 1-C_3H_7O,[19] 1-C_4H_9O,[21] iso-C_4H_9O,[22] and neo-$C_5H_{11}O$.[22]

If the R + O reaction is used for RO production, the general features of the mechanism can be summarized as follows

$$R + O \rightarrow RO^* \quad (a)$$

$$RO^* \rightarrow HCHO + R' \quad (a1)$$

$$RO^* \rightarrow \text{aldehyde} + H \quad (a2)$$

$$R + O \rightarrow OH + \text{alkene} \quad (b)$$

The direct abstraction reaction b is observed with a relative contribution of ca. 25%[14,15,18] if β-hydrogen is present in the alkyl radical (absent e.g., in the reaction neo-C_5H_{11} + O[18]). The highly excited intermediate RO* undergoes fast unimolecular decomposition by β-C−C and β-C−H bond scission, where isomerization followed by dissociation cannot compete effectively.[14,15,17] It is interesting to investigate whether cyclic and open-chain radicals show different channel branching due to ring-strain effects. To this end c-C_5H_9O is a suitable candidate because it is experimentally easily accessible yet small enough to show a not too complex product spectrum.

A number of studies on thermal cyclopentoxy radical reactions are published. They were mostly performed in solution, and the early works are briefly reviewed in ref 23. Ring cleavage was shown to be the dominating reaction path, and in ref 23, an activation energy of 60.5 kJ/mol was calculated on the AM1-UHF level. From group additivity, a value of −12.5 kJ/mol for the enthalpy of reaction was estimated (AM1-UHF = −13.2 kJ/mol), and reversibility of the ring-opening reaction was considered for the first time.[23] In a more recent theoretical work, Wilsey et al.[24] obtained a threshold energy of 64.4 kJ/mol from CASSCF/6-31G* computations and an energy of reaction of −18.0 kJ/mol (potential-energy differences, zero-point energies not included). In an experimental study on the Cl-atom-initiated oxidation of cyclopentane, a barrier for ring opening in the range 30−35 kJ/mol was deduced.[25] In a most recent work on photodetachment from the c-C_5H_9O anion, ring opening of the c-C_5H_9O radical is also discussed to be an important channel and the dissociation toward C_2H_4 + CH_2CH_2CHO was determined to be energetically nearly neutral (−12 ± 12 kJ/mol).[26] To our knowledge, no information on unimolecular reactions of c-C_5H_9O other than ring opening are available to date.

If c-C_5H_9O* is produced in the c-C_5H_9 + O reaction, it bears an excess energy of about 380 kJ/mol (see below), and competing as well as consecutive reaction pathways are open. The conceivable reaction channels are represented in the following scheme (an asterisk denotes chemical activation)

$$\text{c-}C_5H_9 + O \rightarrow \text{c-}C_5H_9O^* \quad (1a)$$

$$\text{c-}C_5H_9O^* \rightarrow \text{c-}C_5H_8O + H \quad (1a1)$$

$$\rightarrow \bullet CH_2(CH_2)_3CHO^* \quad (1a2)$$

$$\bullet CH_2(CH_2)_3CHO^* \rightarrow CH_2CH(CH_2)_2CHO + H \quad (1a3)$$

$$\rightarrow 2C_2H_4 + H + CO \quad (1a4)$$

$$\rightarrow C_3H_4O + C_2H_4 + H \quad (1a5)$$

$$\text{c-}C_5H_9 + O \rightarrow OH + \text{c-}C_5H_8 \quad (1b)$$

Other cyclic structured molecules such as cyclobutane and methyl cyclobutanone are energetically accessible, too. The objectives and methods of the present study are:

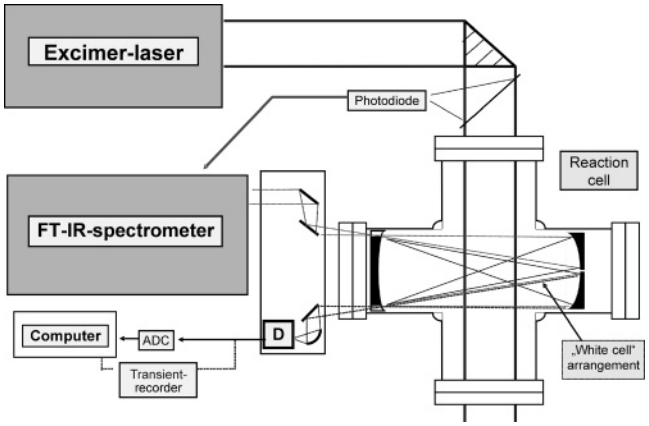

Figure 1. Experimental arrangement A. For explanation, see text. D: detector.

(i) the determination of the branching ratio (1a)/(1b),

(ii) the determination of the relative yields for the cannels $1a_1$−$1a_5$ by using quantitative Fourier transform infrared (FTIR) spectroscopy in a laser-flash photolysis arrangement,

(iii) the determination of the rate coefficient for the reaction c-C_5H_9 + O → products from the specific and sensitive detection of radicals by multiphoton ionization mass spectrometry in combination with a conventional fast flow reactor, and

(iv) analysis of the experimental results in terms of statistical rate theory and quantum chemical calculations.

Experimental Section

Two different experimental arrangements have been used: Arrangement A is a laser-flash photolysis setup directly coupled to a FTIR spectrometer for the identification and quantification of stable species. Arrangement B is a discharge flow reactor coupled to a time-of-flight (TOF) mass spectrometer with laser-induced multiphoton ionization for the detection of hydrocarbon radicals. As details of the experimental setups are presented elsewhere[22,27] only the essentials are given here.

Arrangement A. The setup consists of three major modules: the reaction cell, the excimer laser, and the FTIR spectrometer. A scheme is given in Figure 1.

The laser-flash photolysis cell (pressure = 4 mbar) is equipped with an internal classical "White cell" arrangement in order to realize a long optical path length; within the reaction cell, the IR beam is reflected 32 times, corresponding to a path length of 7 m. The MCT detector enables time-resolved measurements with a time resolution of ≥5 μs in the "step scan" modus. In the present study, the short response time of the detector is useful to enhance data acquisition and averaging, whereby the FTIR spectrometer (Bruker, IFS 66) can be operated in the fastest mode without a decrease in signal-to-noise ratio (highest mirror frequency in the Michelson interferometer). The determination of absolute concentrations is accomplished by calibration. The calibration measurements of the pure substances were performed with partial pressures ranging from 0.01 to 0.1 mbar at the actual pressure of the experiment and using the same bath gas. For some species, time-dependent effects (adsorption on mirrors, condensation) were observed in the calibration procedures and hence had to be accounted for in the product analysis routines.

The output of a single laser shot (Lambda Physik, Compex 102) is around 120 mJ before entering the reaction cell. The number of laser shots per reaction mixture did not exceed 400 (corresponding to a conversion about 15%) to limit secondary photolysis of products.

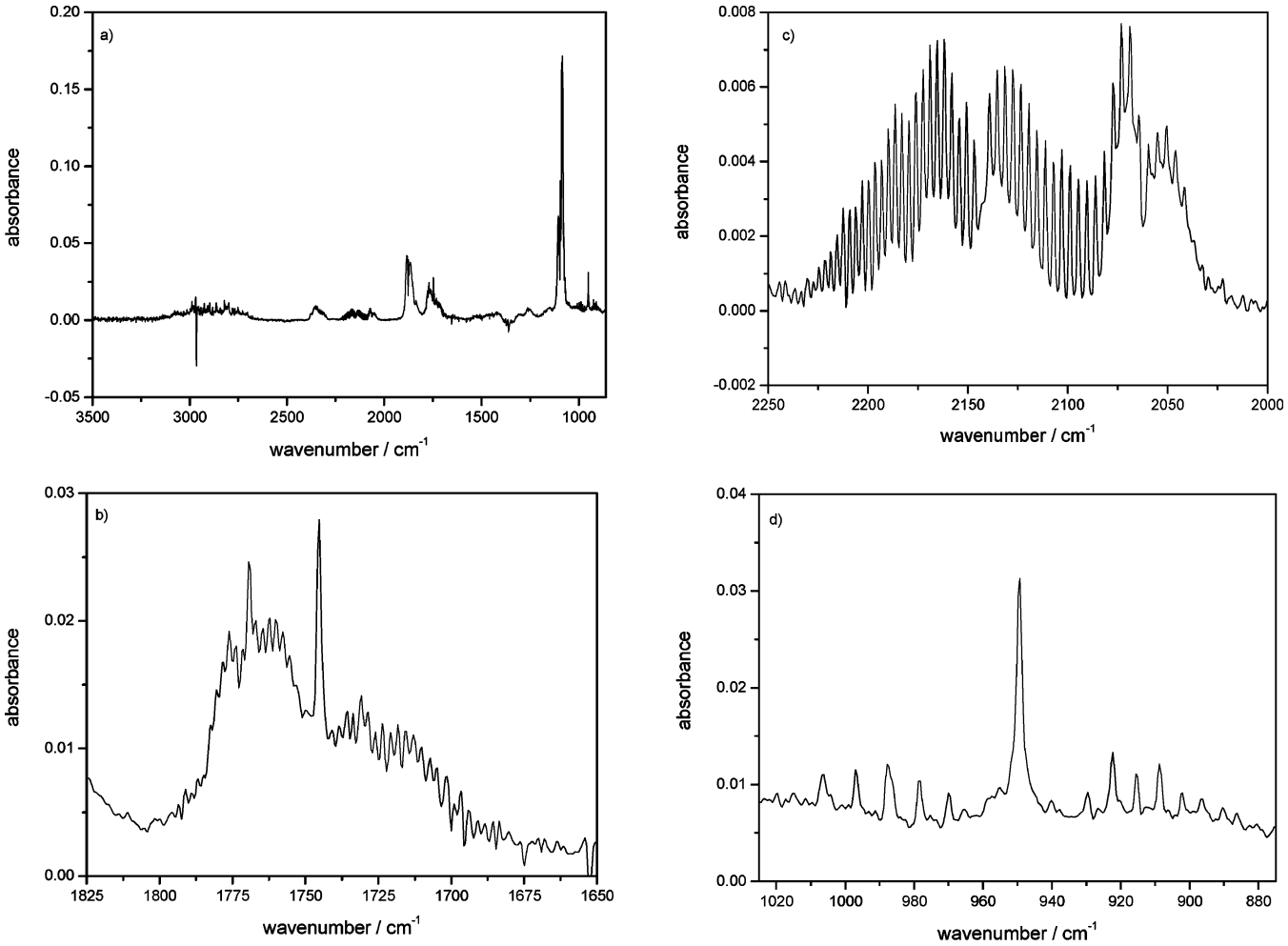

Figure 2. The reaction c-C5H_9+ O: (a) reaction spectrum after subtraction of the contributions from precursors; (b−d) expanded spectra of carbonyl bands, CO, and C_2H_4, respectively. The rotational resolution of CO displayed in c is superimposed byproducts of the side reaction $CFCl_3$ + SO_2. Conditions: p = 4 mbar, T = 298 K, p(c-C_5H_{10}) = 0.2 mbar, p(SO_2) = 0.1 mbar, p($CFCl_3$) = 0.2 mbar, bath gas Ar.

The labile species c-C_5H_9 and O are generated from the precursors c-C_5H_{10}, SO_2, and $CFCl_3$ by cophotolysis at 193 nm. The consumption of the precursor c-C_5H_{10} is determined and all C atom containing substances are identified and quantified. In all experiments the recovery of the total carbon mass is above 90%.

Arrangement B. A conventional discharge flow reactor is coupled to the ion source of a TOF mass spectrometer via a molecular beam inlet. The radicals c-C_5H_9, C_2H_5, and CH_2OCH_3 are produced from c-C_5H_{10}, C_2H_6, and CH_3COCH_3, respectively, by reaction with atomic fluorine produced from highly diluted F_2/He mixtures in a microwave discharge. The O atoms are produced from highly diluted O_2/He mixtures via a microwave discharge. The O atom concentration is accessible from the degree of dissociation of O_2. The radicals are detected after laser-induced multiphoton ionization at λ = 433 nm. This wavelength was found to be appropriate for the simultaneous detection of all three radicals.

Chemicals. Chemicals were used without any further purification: He (≥99.995%), Ar (≥99.998%), SO_2 (≥99.98%), CO (≥98%), He/F_2 (≥99.995/98%), C_2H_4 (≥99.9), all Messer-Griesheim; c-C_5H_{10} (≥99.8%), Merck; $CFCl_3$ (≥99.5%), C_3H_4O (≥95%), c-C_5H_8O (≥99%), all Fluka; $CH_2CH(CH_2)_2CHO$ (≥97%), $CH_3CH_2(CH)_2CHO$ (≥95%), all Lancaster; c-C_5H_8 (≥96%), Aldrich.

Results and Discussion

Identification of Primary Products. For the identification of the stable products, the IR spectra were analyzed in the range of 600−3500 cm^{-1}. For the quantification of the precursor consumption and product formation, regions with minimal spectral interference from different species were chosen. For most species, the selection of characteristic peaks or rotationally resolved spectra allowed an unambiguous identification. Figure 2 shows an example of a reaction spectrum and displays spectral regions where products have been observed. The spectra were corrected for the consumption of the precursors.

The identification of the product cyclopentene is displayed in Figure 3. The identification was not simply based on one single characteristic peak but on the spectral range 2940−2800 cm^{-1}. Here a number of small absorption peaks and the characteristic shape clearly show the formation of cyclopentene. In this region, the identification is complicated by a high background, which results from an unavoidable signal from water and from HCHO produced by the reaction.

Figure 4 shows an enlarged cutout from the IR spectrum in the region of 1840−1660 cm^{-1}. The spectra of the precursors and of HCHO have been corrected. The identification of three carbonyl substances was accomplished by comparing the reaction spectrum with the spectra of pure substances in the range of 1840−1660 cm^{-1}. Cyclopentanone is assigned on the

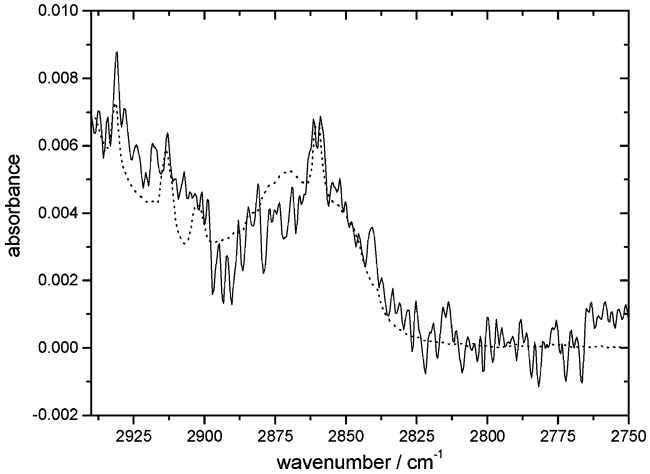

Figure 3. The reaction c-C_5H_9 + O: Identification of cyclopentene. The figure shows the modified reaction spectrum (straight line) after subtraction of c-C_5H_{10}, ethene, and carbonyl containing compounds and the spectrum of cyclopentene (dotted line).

basis of the peak at 1769 cm^{-1}. 4-Pentenal could be unambiguously identified by a supplemental comparison of the spectra in the range of 2840−2660 cm^{-1} displayed in Figure 5. In general, aldehydes have two characteristic bands at 2900−2800 and 2780−2680 cm^{-1}, resulting from C−H-stretching modes. Acrolein matches exactly the difference of the reaction spectrum and the combined contributions of cyclopentanone and 4-pentenal in both spectral position and intensity. Figure 4b shows that the sum of the pure cyclopentanone, 4-pentenal, and acrolein spectra is in very good agreement with the reaction spectrum. The residuum demonstrates that there are no other substances left containing a C═O double bond. Thus, for the c-C_5H_9O + O reaction, the following products have been clearly identified: ethene, cyclopentanone, 4-pentenal, cyclopentene, acrolein, HCHO, and CO.

An Additional Study: The c-C_5H_8 + O Reaction. As cyclopentene (c-C_5H_8) is a product of c-C_5H_9 + O and because c-C_5H_8 + O is fast ($k = 1.27 \times 10^{13}$ cm^3 mol^{-1} s^{-1}),[28] we separately studied the latter reaction to clarify possible interference of common products. In photolysis experiments with c-C_5H_8 in the presence and absence of SO_2 (i.e., O atoms) the reaction products have been determined. Before the interpretation of our results, it is useful to summarize some earlier work of Cvetanović and co-workers (for the mechanism see Figure 6).[29] These authors suggested formation of an O- and C-centered triplet diradical, for the decomposition of which different pathways are conceivable: (i) formation of cyclopentene oxide by ring closure; (ii) 1,2 hydrogen shift to form cyclopentanone; (iii) 1,2 ring cleavage forming a noncyclic diradical, which may lead by a 1,3 hydrogen shift to 4-pentenal, or by a C−C fission to acrolein and ethene (a direct concerted formation is also possible), and by ring contraction to cyclobutylcarboxaldehyde, respectively.

Our quantitative analysis was made by analysis of the FTIR reaction spectrum following the procedure outlined above. The experimental results are given in Table 1 together with the values from Cvetanović et al. The product yields vary in the channels to cyclopentanone (this work, 29.5%; Cvetanović, 16.3%) and 4-pentenal (5.7%; 0.5%). The other values agree within the experimental error margins; some products mentioned by Cvetanović et al. could not be observed (cyclobutylcarboxyaldehyde and dihydropyran). Because of different absorption bands in the region of the C═O mode (conjugation effect for 2-pentenal results in a red shift of 30 cm^{-1}), an explicit

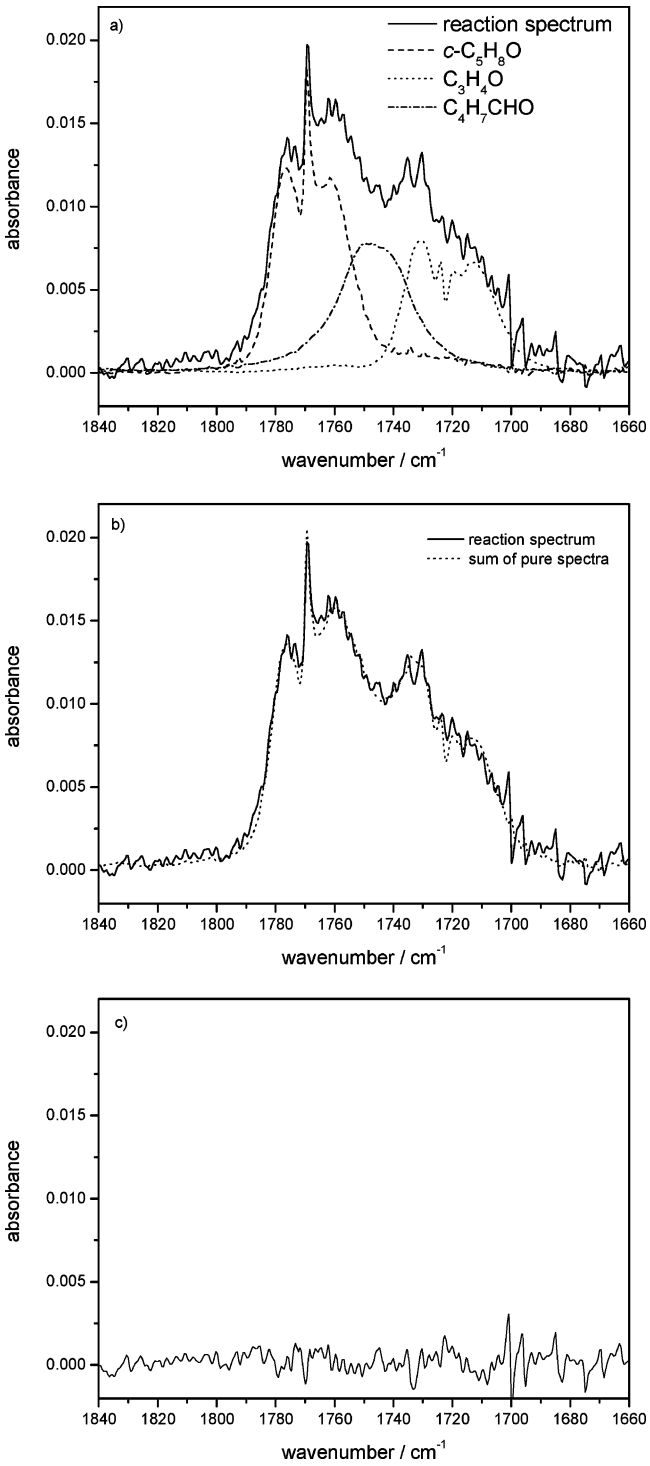

Figure 4. The reaction c-C_5H_9 + O: Identification of carbonyl compounds. (a) Comparison of the reaction spectrum with the spectra of the pure substances; (b) comparison of the reaction spectrum with the sum of pure spectra; (c) residuum.

determination of 2-pentenal and 4-pentenal is possible. The formation of 2-pentenal (neither cis nor trans), discussed by Cvetanović et al., could not be observed. Cvetanović et al., reporting an appreciable scatter in the yields of cyclopentanone and cyclobutylcarboxyaldehyde, attributed the loss of these highly polar substances to reactions at the incompletely coated stainless steel column. The loss of highly polar substances at the stainless steel wall has been observed in our work for long residence times, too. However these effects from different

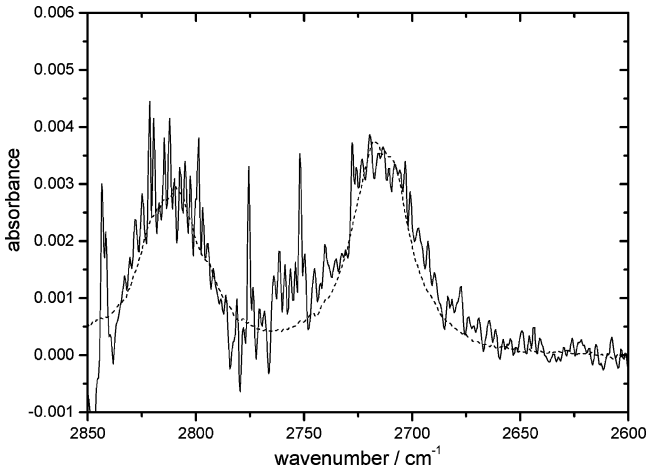

Figure 5. The reaction c-C_5H_9 + O: Comparison of the reaction spectrum (straight line) and 4-pentenal spectrum (dotted line).

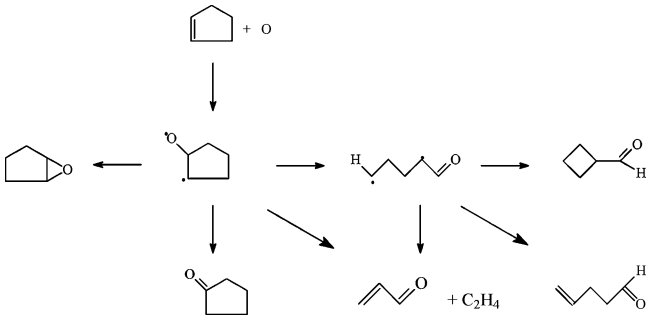

Figure 6. Scheme for the reaction c-C_5H_8 + O.

TABLE 1: Product Yields[a] for Reaction c-C_5H_8 + O

substance	this work	Cvetanović
ethane	23.9%	18.6%
acrolein	18.2%	20.9%
cyclopentanone	29.5%	16.3%
cyclopentenoxide	22.7%	36.0%
4-pentenal	5.7%	0.5%
cyclobutylcarboxaldehyde	0%	7.0%
dihydropyran	0%	0.7%

[a] Experimental conditions: This work: p_{total} = 4 mbar, p(c-C_5H_8) = 0.02 mbar, T = 298 K; Cvetanović:[29] p_{total} = 36 mbar, p(c-C_5H_8) = 1.6 mbar. (The original values of Cvetanović are multiplied by a factor of 1.16 in order to give a total product yield of 100%; the values for cyclopentanone and cyclobutylcarboxyaldehyde are reported as approximate.)

volatility and from condensation have been taken into account in our work in the calibration procedures.

Quantitative Analysis of Products. The product yields were calculated from the total product concentrations according to the reaction mechanism 1a...1b shown above. The contribution of the reaction $1a_4$ was determined based on its ethylene yield calculated as follows $[C_2H_4]_{(1a_4)} = ([C_2H_4]_{abs} - [C_3H_4O]_{abs})/2$, where $[C_2H_4]_{abs}$ and $[C_3H_4O]_{abs}$ denote the absolute concentrations of ethene and acrolein, respectively.

We note that the ratio [cyclopentanone]/[4-pentenal] was observed to depend on $[SO_2]$, that is, on the concentration of oxygen atoms. High concentrations lead to ratios larger than 1, and low oxygen concentrations to ratios lower than 1; this is displayed in Figure 7. The limit extrapolated for $[SO_2]_0 \rightarrow 0$ corresponds to yields with negligible contributions from secondary reactions.

For the relative branching fractions of reactions 1a and 1b, we obtained values of 68 ± 5 and 32 ± 4%, respectively. The

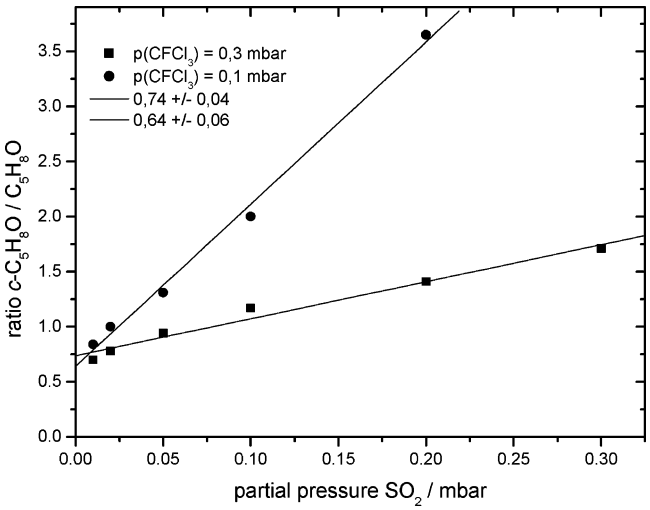

Figure 7. The reaction c-C_5H_9 + O: Ratio [c-C_5H_8O]/[C_4H_7CHO] vs oxygen precursor concentration $[SO_2]$, 400 laser shots, total pressure = 4 mbar.

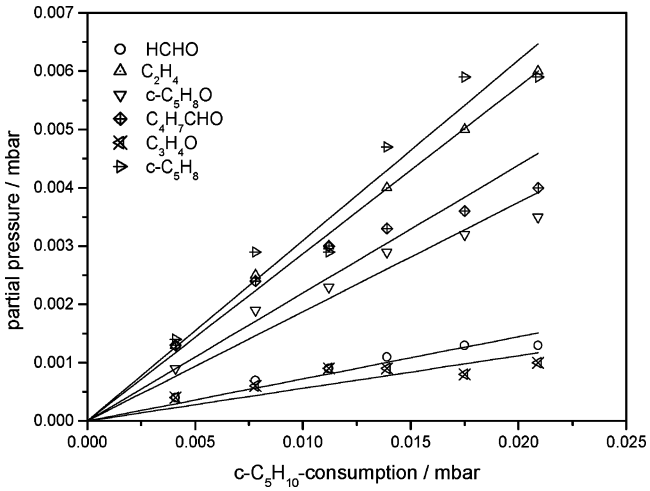

Figure 8. The reaction c-C_5H_9 + O: Partial pressures of primary products as a function of the c-C_5H_{10} consumption. Conditions: p(c-C_5H_{10}) = 0.1 mbar, $p(SO_2)$ = 0.01 mbar, $p(CFCl_3)$ = 0.3 mbar, p_{total} = 4 mbar; T = 298 K.

error margins reflect the estimated uncertainties from the calibration of the concentrations and from the matching of the spectra for the pure substances and reaction products. The pathway to cyclopentene may be higher than specified, because secondary reactions mainly with oxygen atoms may lead to a loss of cyclopentene. An underestimation of the pathway to cyclopentene can be minimized by the above mentioned use of oxygen-deficient initial conditions. The quantitative detection of stable products leads to the following relative branching fractions for the decomposition of the cyclopentoxy radical: $(1a_2)/(1a_1) = (47 \pm 5)/(21 \pm 2)$. The ring cleavage reaction $(1a_2)$ is the major pathway, but the direct hydrogen split off, reaction $(1a_1)$, leading to cyclopentanone seems to be relevant, too. For the further decomposition steps of the open-chain 4-formylbutyl radical, the following relative yields were obtained: $(1a_3)/(1a_4)/(1a_5) = (27 \pm 2)/(12 \pm 2)/(8 \pm 1)$. The product yields do not depend on the consumption of the precursor, c-C_5H_{10} as is illustrated in Figure 8. In Figure 9 the pathways for the decomposition of the chemically activated cyclopentoxy radical are summarized in some detail.

Our findings are to be compared with four previous studies. Takagi et al.[30] reported the formation of cyclopentanone in their

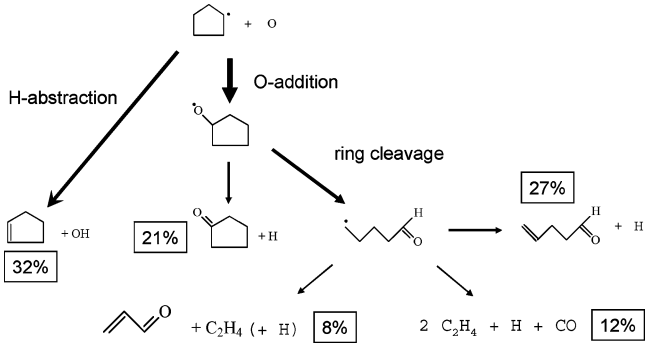

Figure 9. Scheme of the reaction c-C_5H_9 + O.

work on the photo-oxidation of c-C_5H_{10} in an NO/H_2O/air system, which is a complex reaction system with respect to the elucidation of products of an elementary reaction. Heinemann-Fiedler et al.[31] investigated the reaction c-C_5H_9 + O by mass spectrometry and observed the main products cyclopentanone and cyclopentene. But because of mass spectrometric interferences, the identification of other products and a precise determination of product yields was out of place. As mentioned above, Orlando et al.[25] exclusively discuss ring opening as further reactions of the c-C_5H_9O radical.

Rate of Reaction. By use of the experimental setup B, the rate coefficient of the c-C_5H_9 + O reaction was measured with reference to the reaction C_2H_5 + O and with reference to the reaction of CH_3OCH_2 + O. The determination of the rate coefficient was based on the relative rate technique for 2 competing reactions

$$R_1 + O \rightarrow \text{products} \qquad \text{(i)}$$

$$R_2 + O \rightarrow \text{products} \qquad \text{(ref)}$$

The kinetics of two simultaneous reactions leads to the relation

$$k_{rel} = k_i/k_{ref} = \ln\{[R_1]_0/[R_1]\}/\ln\{[R_2]_0/[R_2]\}$$

where $[R_i]_0$ and $[R_i]$ are the concentrations of the radical R_i in absence and presence of O atoms, respectively. To ensure that other reactions such as radical−radical self-reactions, radical cross reactions, and secondary reactions with oxygen atoms do not interfere, very low absolute radical concentrations have to be used.

For the competing reactions *c*-C_5H_9 + O/C_2H_5 + O the ratio k_{rel} = *k*(c-C_5H_9 + O)/*k*(C_2H_5 + O) = 1.67 ± 0.15 was determined; this is illustrated in Figure 10. With the well-known[19] rate coefficient *k*(C_2H_5 + O) = 1.04 × 10^{14} cm^3 mol^{-1} s^{-1}, it follows for the absolute value *k*(c-C_5H_9 + O) = (1.73 ± 0.16) × 10^{14} cm^3 mol^{-1} s^{-1}. A second determination of the rate coefficient by the competitive reaction with methoxymethyl radicals adopting[32] *k*(CH_3OCH_2 + O) = (1.31 ± 0.08) × 10^{14} cm^3 mol^{-1} s^{-1} leads to *k*(c-C_5H_9 + O) = (1.73 ± 0.05) × 10^{14} cm^3 mol^{-1} s^{-1} in perfect agreement to the above result.

In a former study[31] by using a Laval nozzle reactor with mass spectrometric detection of the radicals, the rate of reaction for c-C_5H_9 + O was measured with reference to CH_3 +O leading to *k*(c-C_5H_9 + O)/*k*(CH_3 + O) = 2.02. By adoption of a recent value[27] of *k*(CH_3 + O) = 7.6 × 10^{13} cm^3 mol^{-1} s^{-1}, this gives *k*(c-C_5H_9 + O) = 1.54 × 10^{14} cm^3 mol^{-1} s^{-1}. In another study of the title reaction by a similar arrangement (fast flow reactor/multiphoton ionization mass spectrometer), the reaction C_2H_5 + O was used as the competing reference reaction.[33] The

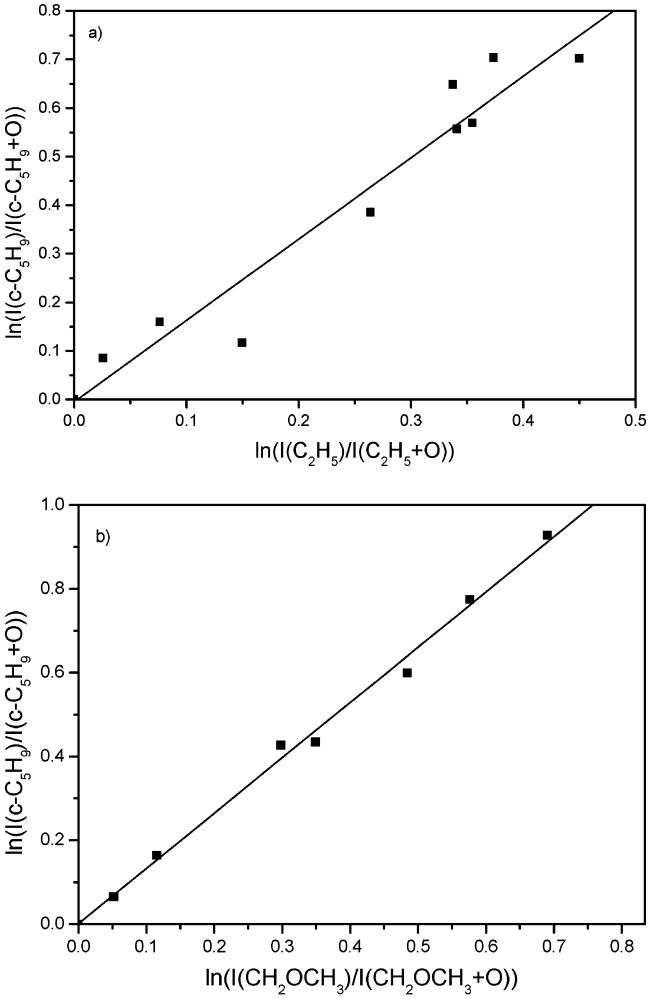

Figure 10. The reactions c-C_5H_9/C_2H_5 + O and c-C_5H_9/CH_2OCH_3 + O: Determination of the relative rate coefficients of the reactions (a) c-C_5H_9 + O vs C_2H_5 + O and (b) c-C_5H_9 + O vs CH_2OCH_3 + O by the consumption of the radicals for increasing amounts of O atoms. Conditions: arrangement B, λ = 433 nm, laser energy 10 mJ, T = 298 K. (a) p = 2.0 mbar; x(c-C_5H_{10}) = 0.81, x(C_2H_6) = 1.84, x_0(F) = 0.02, x(O) = 0−0.2; unit mol % (b) p = 1.9 mbar, x(c-C_5H_{10}) = 0.90, x(CH_3OCH_3) = 0.42, x_0(F) = 0.02, x(O) = 0−0.2; unit mol %.

reported value of *k*(c-C_5H_9 + O)/*k*(C_2H_5 + O) = 1.5 is transformed via *k*(C_2H_5 + O) = 1.04 × 10^{14} cm^3 mol^{-1} s^{-1} (see above) to *k*(c-C_5H_9 + O) = 1.56 × 10^{14} cm^3 mol^{-1} s^{-1}.

By consideration of the different experimental conditions, the agreement between the values reported so far and the values presented here is good.

Simulation. To assess the contributions of secondary reactions to the measured final product distribution and in order to estimate the error margins of the branching ratios, a full simulation of the concentration−time profiles was performed. On the basis of a moderately complex mechanism with a set of 28 reactions (see Table 2), the oxidation of cyclopentyl radicals initiated by O atoms was simulated. For the reaction c-C_5H_9 + O the kinetic data determined in the present work were used. The initial concentrations of O and Cl atoms are accessible via the absorption coefficients of SO_2 and $CFCl_3$ and the laser energy absorbed within the reaction cell. The initial concentrations derived and used for the simulation are: $[c\text{-}C_5H_{10}]_0$ = 2.0 × 10^{-8} mol/cm^{-3}; $[O]_0$ = 3.4 × 10^{-10} mol/cm^3; $[Cl]_0$ = 5.6 × 10^{-10} mol/cm^3. A plot of the results for the major products is displayed in Figure 11. The relative yields based on the sum of all concentrations of the final products are collected in Table

TABLE 2: Reaction Mechanism for the Determination of the Product Yield for the Reaction of c-C_5H_9 + O[a]

1	$OH + O \rightarrow O_2 + H$	$k = 2.00 \times 10^{13}$
2	$OH + H \rightarrow H_2O$	$k = 1.00 \times 10^{10}$
3	c-$C_5H_9 + O \rightarrow$ c-$C_5H_8 + OH$	$k = 5.54 \times 10^{13}$
4	c-$C_5H_9 + O \rightarrow$ c-$C_5H_8O + H$	$k = 3.63 \times 10^{13}$
5	c-$C_5H_9 + O \rightarrow 2\ C_2H_4 + HCO$	$k = 1.90 \times 10^{13}$
6	$HCO \rightarrow H + CO$	$k = 7.00 \times 10^{14}$
7	c-$C_5H_9 + O \rightarrow C_4H_7CHO + H$	$k = 4.67 \times 10^{13}$
8	c-$C_5H_9 + O \rightarrow C_2H_4 + C_3H_4O + H$	$k = 1.38 \times 10^{13}$
9	c-$C_5H_9 + H \rightarrow$ c-C_5H_{10}	$k = 8.50 \times 10^{12}$
10	c-C_5H_9 + OH → Products	$k = 2.00 \times 10^{13}$
11	c-C_5H_9 + Cl → c-C_5H_8 + HCl	$k = 2.74 \times 10^{14}$
12	c-C_5H_{10} + Cl → c-C_5H_9 + HCl	$k = 1.96 \times 10^{14}$
13	c-$C_5H_{10} + O \rightarrow$ c-$C_5H_9 + OH$	$k = 7.40 \times 10^{10}$
14	c-$C_5H_{10} + H \rightarrow$ c-$C_5H_9 + H_2$	$k = 3.44 \times 10^{09}$
15	c-C_5H_{10} + OH → c-$C_5H_9 + H_2O$	$k = 2.89 \times 10^{12}$
16	c-$C_5H_8 + O \rightarrow$ cyclopentenoxide	$k = 2.50 \times 10^{12}$
17	c-$C_5H_8 + O \rightarrow$ c-C_5H_8O	$k = 3.25 \times 10^{12}$
18	c-$C_5H_8 + O \rightarrow C_2H_4 + C_3H_4O$	$k = 2.00 \times 10^{12}$
19	c-$C_5H_8 + O \rightarrow C_4H_7CHO$	$k = 6.25 \times 10^{11}$
20	c-C_5H_8 + OH → products	$k = 3.40 \times 10^{13}$
21	c-$C_5H_8O + O \rightarrow$ products + OH	$k = 1.07 \times 10^{10}$
22	c-C_5H_8O + OH → products	$k = 1.77 \times 10^{12}$
23	c-C_5H_8O + Cl → products + HCl	$k = 2.86 \times 10^{13}$
24	$C_2H_4 + O \rightarrow$ products	$k = 5.48 \times 10^{11}$
25	$C_2H_4 + H \rightarrow C_2H_3 + H_2$	$k = 2.54 \times 10^{13}$
26	$C_2H_4 + H \rightarrow C_2H_5$	$k = 6.59 \times 10^{11}$
27	C_2H_4 + OH → products	$k = 5.66 \times 10^{12}$
28	$C_2H_3 + H \rightarrow C_2H_4$	$k = 1.21 \times 10^{14}$

[a] Rate coefficients are taken from ref 50. Initial concentrations used for the simulation: $[c\text{-}C_5H_{10}]_0 = 2.0 \times 10^{-8}$ mol/cm^{-3}, $[O]_0 = 3.4 \times 10^{-10}$ mol/cm^3, $[Cl]_0 = 5.6 \times 10^{-10}$ mol/cm^3.

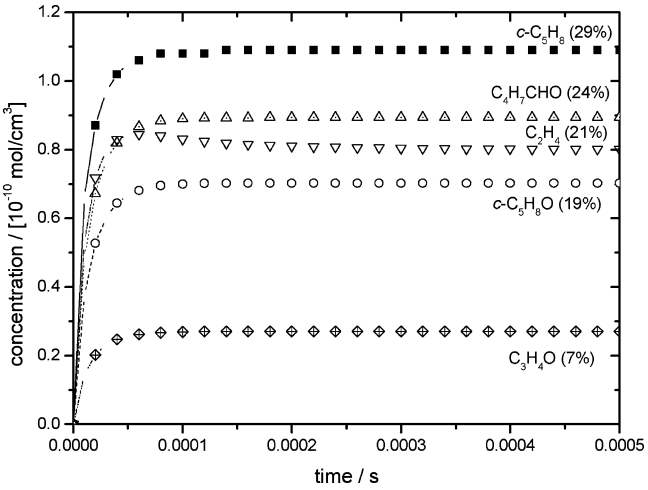

Figure 11. The reaction c-C_5H_9 + O: Simulation of the overall reaction. The concentration of products vs time for the initial concentrations $[c\text{-}C_5H_{10}]_0 = 2.0 \times 10^{-8}$ mol/cm^3, $[O]_0 = 3.4 \times 10^{-10}$ mol/cm^3, $[Cl]_0 = 5.6 \times 10^{-10}$ mol/cm^3.

3 and compared with the experimental results. An inspection shows that secondary reactions modify the primary product distribution only within the given error margins. Therefore, the experimentally derived branching ratios of the product channels are thought to be a good basis for a comparison with theoretically obtained values.

Modeling of the Chemically Activated Decomposition. Apart from the ring-opening reaction ($1a_2$), no thermochemical data for unimolecular reactions of C_5H_9O species are available. Therefore, we calculated energies of intermediates and transition states at G2(MP2) level[34] using the Gaussian 98 program suite.[35] The results are displayed in Figure 12. Inspection shows that the ring-opening reaction with a threshold energy of 32.3 kJ/mol is the dominating pathway. The threshold energy is in good

TABLE 3: Product Yields (mol %) with Respect to the Sum of All Products for Reaction c-C_5H_9 + O

	experiment	simulation[a]
c-C_5H_8	27	29
C_4H_7CHO	23	24
c-C_5H_8O	18	19
C_2H_4	25	21
C_3H_4O	7	7

[a] Simulated final product distribution does not represent channel distributions $1a_1-1a_5$ directly.

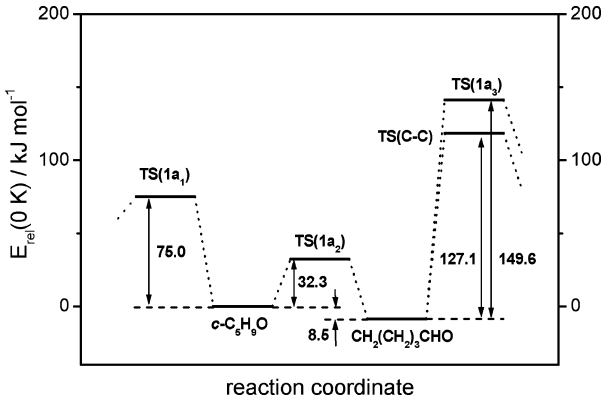

Figure 12. Energy diagram for the unimolecular reactions of C_5H_9O from G2(MP2) calculations; TS(C−C) denotes the first transition state along routes $1a_4$ and $1a_5$, viz., C_2H_4 split off from $CH_2(CH_2)_3CHO$.

agreement with the estimation from ref 25 (30−35 kJ/mol) but lower than the calculated values from ref 23 (60.5 kJ/mol for $T = 298$ K, AM1-UHF) and ref 24 (64.4 kJ/mol, CASSCF/6-31G(d)). We note that the value given in ref 24 is the potential energy difference, which yields $E_0(0\ K) = 54.4$ kJ/mol when corrected with the zero-point energies from the G2(MP2) calculations. For open-chain secondary alkoxy radicals, threshold energies in the range 42−50 kJ/mol are predicted for β-C−C bond breaking with fragments > CH_3.[11,15,36] If the strain energy of a five-membered ring (~25 kJ/mol[37]) is assumed to be partly released in going to the transition state, a threshold energy near 30 kJ/mol for the cyclopentoxy radical seems reasonable.

For the β-C−H bond fission, we obtained a threshold energy of 75.0 kJ/mol. This is similar to the corresponding values of open-chain radicals, for which threshold energies between 70 and 80 kJ/mol were calculated at different quantum chemical levels.[12,36] From the experimental heat of formation of cyclopentanone (−193 kJ/mol[38]) and the value resulting from group additivity,[37] a ring-strain energy of 21 kJ/mol is obtained. This is close to the value for the cyclopentoxy radical (25 kJ/mol, see above), and hence, ring strain is expected only little to change the threshold energy for C−H bond split compared to open-chain radicals.

The ring-opening product of reaction $1a_2$, the 4-formylbutyl radical, essentially represents an alkyl radical, and the threshold energies for β-C−C and β-C−H bond scission, 127.1 and 149.6 kJ/mol, respectively, are typical for alkyl radicals.[39] The most energetically favorable isomerization reaction, the 1,4 H shift, is expected to have a threshold energy around 80 kJ/mol[40] or even a little bit lower due to resonance stabilization of the 1-formylbutyl radical formed. Because of their tight transition states, however, isomerization reactions usually cannot compete with dissociation steps at high energies[21] and, hence, are not considered here.

The enthalpy of formation of the cyclopentoxy radical is not known. From the enthalpy of formation of cyclopentanol (−242.6 kJ/mol[38]) and typical O−H bond dissociation energies

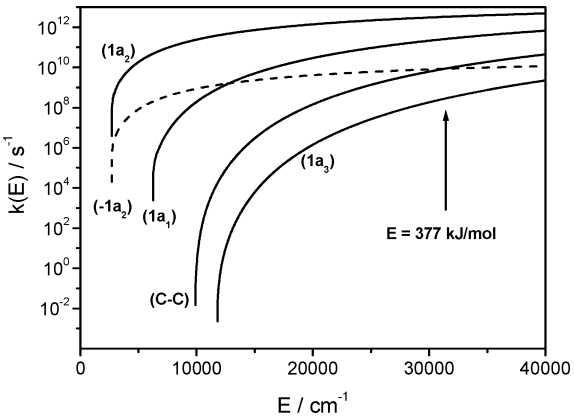

Figure 13. Specific rate coefficients for the unimolecular reactions $1a_1-1a_3$. C−C denotes C_2H_4 split off from $CH_2(CH_2)_3CHO$; arrow = initial excitation energy of c-C_5H_9O; energy zero = rovibrational ground state of c-C_5H_9O.

TABLE 4: Calculated High-Pressure Arrhenius Data and Standard Thermodynamic Parameters for $T = 298$ K[a]

reaction	log(A/s^{-1})	E_a/kJ mol^{-1}
$1a_1$	13.12	77.5
$1a_2$	13.23	35.0
$-1a_2$	11.00	48.6
$1a_3$	12.77	151
C−C	13.66	130
$\Delta_R H°(1a_2) = -13.6$ kJ mol^{-1}		
$\Delta_R S°(1a_2) = 134.1$ J K^{-1} mol^{-1}		

[a] C−C denotes the C_2H_4 split of from $CH_2(CH_2)_3CHO$.

of secondary alcohols (∼440 kJ/mol[41]), a value of −21 kJ/mol can be estimated. Adopting the values for c-C_5H_9 and O atoms from standard tables,[41] we obtain a value of 377 kJ/mol for the initial excitation energy of the chemically activated c-C_5H_9O radical.

For the calculation of branching fractions, we computed specific rate coefficients from RRKM theory[42] using vibrational frequencies (scaled by 0.9472[43]) and rotational constants from ab initio calculations at MP2/6-31G(d) level.[44,45] Densities and sums of states were directly counted[46] for a total angular momentum quantum number $J = 45$,[47] which corresponds to the average rotational excitation of c-C_5H_9O at room temperature. For reactions proceeding via tight transition states; however, this is not a critical parameter. Reaction path degeneracies of 1 where used except for the C−C bond dissociation of $CH_2(CH_2)_3CHO$, where a value of $^1/_2$ was assumed to account for the C_s symmetry of the transition state.[48] The results are shown in Figure 13, and the corresponding high-pressure Arrhenius parameters obtained from simple canonical transition state theory[49] are collected in Table 4; thermodynamic parameters for the equilibrium c-$C_5H_9O \leftrightarrow CH_2(CH_2)_3CHO$ are also given.

The specific rate coefficients at 377 kJ/mol read as follows: $k(1a_1) = 2.6 \times 10^{11}$ s^{-1}, $k(1a_2) = 3.3 \times 10^{12}$ s^{-1}, $k(-1a_2) = 8.5 \times 10^{9}$ s^{-1}, $k(1a_3) = 2.9 \times 10^{8}$ s^{-1}, and k(C−C) $= 2.6 \times 10^{9}$ s^{-1}. It is obvious that the equilibrium ($1a_2$) is established on a picosecond time scale with a microscopic equilibrium constant at this energy of $K(1a_2) = 390$. Cyclopentanone formation ($1a_1$) is also fast, and numerical integration with the above specific rate coefficients gives a yield of ∼13%, which is not too far from the experimental value of 31%. We note that integration is necessary here, since equilibration and cyclopentanone formation proceed on a similar time scale. A simple equilibrium approach would underestimate the yield by a factor of ca. 0.5. The remaining 87% account for the decomposition products of $CH_2(CH_2)_3CHO$. Here C−C bond breaking is clearly overestimated (84%) compared with the experimental result (29%); accordingly reaction $1a_3$ is predicted to contribute with 3%, whereas the experimental value is 40%. The rate coefficients of the $CH_2(CH_2)_3CHO$ decomposition reactions are in the order of 10^9 s^{-1}, that is, in the range of the collision number in our experiments. Therefore, collisional deactivation is surely not negligible, and the effective excitation energy of the chemically activated intermediates is below its initial value of 377 kJ/mol. A decreasing energy, however, increases the yield of the cyclopentanone channel ($1a_1$) as is obvious from Figure 13, and at average energies near 200 kJ/mol, the experimental order of magnitude is reproduced. The simple microcanonical picture, however, is not longer valid, and actual molecular populations have to be calculated by an appropriate master equation, which is beyond the scope of the present work. A comparison of the specific rate coefficients for reaction $1a_3$ and the (C−C) channel in Figure 13 reveals, however, that the overestimation of C−C bond fission as compared to the experimental yield would persist. Also would a low-lying 1,4 hydrogen shift lead to products in part identical to those of the (C−C) pathway (e.g., acrolein). Here clearly more work is needed on channel branching in alkyl-type radicals.

Summary

The channel branching of the c-C_5H_9 + O reaction at room temperature and 4 mbar was experimentally studied and rate coefficients were determined. The reaction proceeds in part via a direct hydrogen abstraction and in part via complex formation. The main reaction channel of the intermediate c-C_5H_9O radical is a reversible ring opening in competition to cyclopentanone formation. The ring-opening product decomposes by β-C−C and β-C−H bond dissociation forming 4-pentenal, acrolein, ethene, and carbon monoxide as main products. The channel branching is discussed in terms of statistical unimolecular rate theory based on molecular properties and thermochemical data from quantum chemical calculations. Arrhenius parameters and thermodynamic data are derived.

Acknowledgment. Funding by the Deutsche Forschungsgemeinschaft (European Graduate School: "Microstructural Control in Free-Radical Polymerization") and the Fonds der Chemischen Industrie is gratefully acknowledged. M.O. thanks the Deutsche Forschungsgemeinschaft (SFB 606 "Instationäre Verbrennung: Transportphänomene, Chemische Reaktionen, Technische Systeme").

References and Notes

(1) Buback, M.; Kling, M.; Schmatz, S. *Z. Phys. Chem.* **2005**, *219*.

(2) Warnatz, J.; Maas, U.; Dibble, R. W. *Combustion*; Springer: Heidelberg, 1996.

(3) Hoyermann, K.; Mauss, F.; Zeuch, T. *Phys. Chem. Chem. Phys.* **2004**, *6*, 3824.

(4) Simmie, J. M. *Prog. Energy Combust. Sci.* **2003**, *29* (6), 599.

(5) Dagaut, P. *Phys. Chem. Chem. Phys*. **2002**, *4*, 2079.

(6) Ranzi, E.; Dente, M.; Goldaniga, A.; Bozzano, G.; Faravelli, T. *Prog. Energy Combust. Sci.* **2001**, *27* (1), 99.

(7) Edwards, T. *J. Propuls. Power* **2003**, *19* (6), 1089.

(8) Potter, T. L.; Simmons, K. E. *Total Petroleum Hydrocarbon Criteria Working Group Series, Vol. 2: Comparison of Petroleum Mixtures*; Amherst: Massachusetts, 1998.

(9) Atkinson, R. *Int. J. Chem. Kinet*. **1997**, *29*, 99.

(10) Blitz, M.; Pilling, M. J.; Robertson, S. H.; Seakins, P. W. *Phys. Chem. Chem. Phys*. **1999**, *1*, 73.

(11) Fittschen, C.; Hippler, H.; Viskolcz, B. *Phys. Chem. Chem. Phys*. **2000**, *2*, 1677.

(12) Hippler, H.; Striebel, F.; Viskolcz, B. *Phys. Chem. Chem. Phys*. **2001**, *3*, 2450.
(13) Méreau, R.; Rayez, M.-T.; Caralp, F.; Rayez, J.-C. *Phys. Chem. Chem. Phys*. **2000**, *2*, 3765.
(14) Méreau, R.; Rayez, M.-T.; Caralp, F.; Rayez, J.-C. *Phys. Chem. Chem. Phys*. **2003**, *5*, 4828.
(15) Somnitz, H.; Zellner, R. *Phys. Chem. Chem. Phys*. **2000**, *2*, 1899.
(16) Buback, M.; Kling, M.; Schmatz, S.; Schröder, S. *Phys. Chem. Chem. Phys*. **2004**, *6*, 5441.
(17) Slagle, I. R.; Sarzynski, D.; Gutman, D.; Miller, J. A.; Melius, C. F. *J. Chem. Soc., Faraday Trans.* **1988**, *84*, 491.
(18) Hoyermann, K.; Olzmann, M.; Seeba, J.; Viskolcz, B. *J. Phys. Chem. A* **1999**, *103*, 5692.
(19) Hoyermann, K.; Olzmann, M.; Zeuch, T. *Proc. Combust. Inst*. **2002**, *29*, 1247.
(20) Harding, L. B.; Klippenstein, S. J.; Georgievskii, Y. *Proc. Combust. Inst*. **2005**, *30*, 985.
(21) Hack, W.; Hoyermann, K.; Kersten, C.; Olzmann, M.; Viskolcz, B. *Phys. Chem. Chem. Phys.* **2001**, *3*, 2365.
(22) Hack, W.; Hoyermann, K.; Olzmann, M.; Viskolcz, B.; Wehmeyer, J.; Zeuch, T. *Proc. Combust. Inst.* **2005**, *30*, 1005.
(23) Beckwith, A. L. J.; Hay, B. P. *J. Am. Chem. Soc*. **1989**, *111*, 230.
(24) Wilsey, S.; Dowd, P.; Houk, K. N. *J. Org. Chem*. **1999**, *64*, 8801.
(25) Orlando, J. J.; Iraci, L. T.; Tyndall, G. S. *J. Phys. Chem. A* **2000**, *104*, 5072.
(26) Alconcel, L. S.; Continetti, R. E. *Chem. Phys. Lett.* **2002**, *366*, 642.
(27) Hack, W.; Hold, M.; Hoyermann, K.; Wehmeyer, J.; Zeuch, T. *Phys. Chem. Chem. Phys.* **2005**, *7*, 1977.
(28) Cvetanović, R. J. *J. Phys. Chem. Ref. Data* **1987**, *16*, 261.
(29) Cvetanović, R. J.; Ring, D. F.; Doyle, L. C. *J. Phys. Chem*. **1971**, *75*, 3056.
(30) Takagi, H.; Washida, N.; Bandow, H.; Akimoto, H.; Okuda, M. *J. Phys. Chem*. **1981**, *85*, 2701.
(31) Heinemann-Fiedler, P.; Hoyermann, K.; Rohde, G. *Ber. Bunsen-Ges. Phys. Chem*. **1990**, *94*, 1400.
(32) Hoyermann, K.; Nacke, F. *Proc. Combust. Inst*. **1996**, *26*, 505.
(33) Rohde, G. Ph.D. Thesis, Göttingen, 1991.
(34) Curtiss, L. A.; Raghavachari, K.; Pople, J. A. *J. Chem. Phys.* **1993**, *98*, 1293.
(35) Frisch, M. J.; Trucks, G. W.; Schlegel, H. B.; Scuseria, G. E.; Robb, M. A.; Cheeseman, J. R.; Zakrzewski, V. G.; Montgomery, J. A., Jr.; Stratmann, R. E.; Burant, J. C.; Dapprich, S.; Millam, J. M.; Daniels, A. D.; Kudin, K. N.; Strain, M. C.; Farkas, O.; Tomasi, J.; Barone, V.; Cossi, M.; Cammi, R.; Mennucci, B.; Pomelli, C.; Adamo, C.; Clifford, S.; Ochterski, J.; Petersson, G. A.; Ayala, P. Y.; Cui, Q.; Morokuma, K.; Malick, D. K.; Rabuck, A. D.; Raghavachari, K.; Foresman, J. B.; Cioslowski, J.; Ortiz, J. V.; Baboul, A. G.; Stefanov, B. B.; Liu, G.; Liashenko, A.; Piskorz, P.; Komaromi, I.; Gomperts, R.; Martin, R. L.; Fox, D. J.; Keith, T.; Al-Laham, M. A.; Peng, C. Y.; Nanayakkara, A.; Gonzalez, C.; Challacombe, M.; Gill, P. M. W.; Johnson, B. G.; Chen, W.; Wong, M. W.; Andres, J. L.; Head-Gordon, M.; Replogle, E. S.; Pople, J. A. *Gaussian 98*, revision A.7; Gaussian Inc.: Pittsburgh, PA, 1998.
(36) Rauk, A.; Boyd, R. J.; Boyd, S. L.; Henry, D. J.; Radom, L. *Can. J. Chem.* **2003**, *81*, 431.
(37) Benson, S. W. *Thermochemical Kinetics*, 2nd ed.; Wiley: New York, 1976.
(38) Cox, J. D.; Pilcher, G. *Thermochemistry of Organic and Organometallic Compounds*; Academic Press: London, 1970.
(39) Tsang, W. *J. Am. Chem. Soc.* **1985**, *107*, 2872.
(40) Viskolcz, B.; Lendvay, G.; Seres, L. *J. Phys. Chem. A* **1997**, *101*, 7119.
(41) *CRC Handbook of Chemistry and Physics*, 75th ed.; CRC Press: Boca Raton, 1994.
(42) Marcus, R. A.; Rice, O. K. *J. Phys. Colloid Chem.* **1951**, *55*, 894. Marcus, R. A. *J. Chem. Phys.* **1952**, *20*, 359.
(43) Scott, A. P.; Radom, L. *J. Phys. Chem.* **1996**, *100*, 16502.
(44) Møller, C.; Plesset, M. S. *Phys. Rev.* **1934**, *46*, 618.
(45) Hehre, W. J.; Radom, L.; v.R. Schleyer, P.; Pople, J. A. *Ab Initio Molecular Orbital Theory*; Wiley: New York, 1986.
(46) Beyer, D.; Swinehart, D. F. *Commun. Assoc. Comput. Mach.* **1973**, *16*, 379; Astholz, D. C.; Troe, J.; Wieters, W. *J. Chem. Phys.* **1979**, *70*, 5107.
(47) Troe, J. *J. Chem. Phys.* **1983**, *79*, 6017; Olzmann, M.; Troe, J. *Ber. Bunsen-Ges. Phys. Chem.* **1994**, *98*, 1563.
(48) Gilbert, R. G.; Smith, S. C. *Theory of Unimolecular and Recombination Reactions*; Blackwell: Oxford, 1990.
(49) Glasstone, S.; Laidler, K. J.; Eyring, H. *The Theory of Rate Processes*; McGraw-Hill: New York, 1941.
(50) NIST, *Chemical Kinetics Database on the Web, Standard Reference Database 17*, Version 7.0, Release 1.3, 2005.